

Negative ions of nitroethane and its clusters

S. T. Stokes,¹ K. H. Bowen,^{1,a)} T. Sommerfeld,² S. Ard,³ N. Mirsaleh-Kohan,³ J. D. Steill,³ and R. N. Compton³

¹Department of Chemistry, Johns Hopkins University, Baltimore, Maryland 21218, USA

²Department of Chemistry, Southeastern Louisiana University, Hammond, Louisiana 70402, USA

³Department of Physics, and Department of Chemistry, The University of Tennessee, Knoxville, Tennessee 37996, USA

(Received 7 September 2007; accepted 7 July 2008; published online 12 August 2008)

Valence and dipole-bound negative ions of the nitroethane (NE) molecule and its clusters are studied using photoelectron spectroscopy (PES), Rydberg electron transfer (RET) techniques, and *ab initio* methods. Valence adiabatic electron affinities (EA_{as}) of NE, $C_2H_5NO_2$, and its clusters, $(C_2H_5NO_2)_n$, $n=2-5$, are estimated using vibrationally unresolved PES to be 0.3 ± 0.2 eV ($n=1$), 0.9 ± 0.2 eV ($n=2$), 1.5 ± 0.2 eV ($n=3$), 1.9 ± 0.2 eV ($n=4$), and 2.1 ± 0.2 eV ($n=5$). These energies were then used to determine stepwise anion-neutral solvation energies and compared with previous literature values. Vertical detachment energies for $(C_2H_5NO_2)_n^-$ were also measured to be 0.92 ± 0.10 eV ($n=1$), 1.63 ± 0.10 eV ($n=2$), 2.04 ± 0.10 eV ($n=3$), and 2.3 ± 0.1 eV ($n=4$). RET experiments show that Rydberg electrons can be attached to NE both as dipole-bound and valence bound anion states. The results are similar to those found for nitromethane (NM), where it was argued that the diffuse dipole state act as a “doorway state” to the more tightly bound valence anion. Using previous models for relating the maximum in the RET dependence of the Rydberg effective principle number n_{max}^* , the dipole-bound electron affinity is predicted to be ~ 25 meV. However, a close examination of the RET cross section data for NE and a re-examination of such data for NM finds a much broader dependence on n^* than is seen for RET in conventional dipole bound states and, more importantly, a pronounced ℓ dependence is found in n_{max}^* (n_{max}^* increases with ℓ). *Ab initio* calculations agree well with the experimental results apart from the vertical electron affinity value associated with the dipole bound state which is predicted to be 8 meV. Moreover, the calculations help to visualize the dramatic difference in the distributions of the excess electron for dipole-bound and valence states, and suggest that NE clusters form only anions where the excess electron localizes on a single monomer. © 2008 American Institute of Physics. [DOI: 10.1063/1.2965534]

I. INTRODUCTION

Nitroethane is a colorless oily liquid at standard temperature and pressure, and it is utilized in a variety of applications (fuel additive, propellant, solvent, and pharmaceutical precursor) at the rate of over 10^6 lb per year in the United States alone. Electron attachment reactions for nitroethane have been reported previously in three low pressure studies, where only dissociative electron attachment was observed.¹⁻³ While all three studies reported the observation of NO_2^- , O^- , OH^- , CN^- , and CNO^- fragment anions, the $C_2H_3NO_2^-$ anion was observed in two of these studies,^{1,3} and the $CH_2NO_2^-$ fragment was recorded in one of them.² Also of interest, Pelc *et al.*¹ reported the formation of HCN^- and NO^- . Calculations by Pacansky *et al.*⁴ predict that the valence electron affinity for HCN is negative (~ -1.95 eV), thus we suggest that the HCN^- observed in the experimental study by Pelc *et al.*¹ can be attributed to either the formation of a long-lived anion with poor Franck-Condon overlap with the ground state, or the formation of a dipole bound anion.⁵ The latter possibility seems to be the more reasonable option since the calculations⁴ also show that HCN^- is bent ($\sim 121.7^\circ$) and extended in bond length relative to HCN.

Low energy electron scattering has also been examined for the series, nitromethane, nitroethane, and nitrobenzene.⁶ The dipole moments for CH_3NO_2 , $C_2H_5NO_2$, and $C_6H_5NO_2$ are 3.46, 3.23, and 4.22 D, respectively. Absolute total integral and total backward-scattering cross sections for these molecules were compared to predictions by the Born point-dipole approximation for the rotationally inelastic scattering cross section for polar molecules. Large cross sections are seen for CH_3NO_2 and $C_2H_5NO_2$, although these monotonically decrease with increasing electron energy above zero. The experimental cross sections generally agree with theory founded on the Born model, however, the Born model significantly underestimates the backward-scattering cross section. The cross section for nitrobenzene shows a pronounced “dip” in the total integral scattering cross section at energies less than ~ 200 meV and centered at ~ 100 meV, although this feature does not appear in the backward-scattering cross section. The feature may be due to an interference of a temporary negative ion state with the continuum. In those studies, the total scattering cross section includes *both* the non-dissociative and dissociative attachment cross sections. Later reference will be made to this study in the calculation of the autodetachment lifetimes for $CH_3NO_2^{-*}$ and $C_2H_5NO_2^{-*}$.

^{a)}Electronic mail: kitbowen@jhu.edu.

formed under low energy unimolecular electron attachment conditions.

Both nitromethane⁷ and nitrobenzene⁸ are well known to capture slow electrons to form negative ions through nuclear excited Feshbach resonances. Nondissociative electron attachment to nitrobenzene forms long-lived negative ions, which can be observed in a mass spectrometer with an auto-detachment lifetime originally reported to be 40 μs ,⁸ although later more precise measurements gave 17.5 μs .⁹

Nitromethane attaches electrons with a lifetime below a few microseconds and its anion is not observed in mass spectrometers under low pressure conditions. We postulate that the same situation holds for the nitroethane molecule. Thermal electron attachment to nitromethane has been attributed to three-body collisional stabilization in a swarm experiment⁷ consistent with the Bloch–Bradbury mechanism. $\text{C}_2\text{H}_5\text{NO}_2^-$ ions formed in the photoelectron spectroscopy (PES) as well as in the Rydberg electron transfer (RET) experiments reported herein are also postulated to be stabilized by collisions and relaxed to low internal energy. In the PES experiments, the background gas provides the third body whereas in the RET experiments the Rb^+ ion core provides the collisional relaxation mechanism.

Rydberg charge transfer reactions with nitromethane and nitrobenzene have been reported.^{10,11} Both valence and dipole bound anions¹² are observed under RET reactions. The results of these experiments suggested that the transfer of a Rydberg electron into a dipole bound anion acts as a “doorway” state to the more stable valence anion state. The anion shows a superposition of a dipole-valence bound electron, in which the system spends most of its time in the valence anion configuration until collisions or radiation remove vibrational excitation in order to further stabilize the anion. One of us has performed high level *ab initio* calculations which support the idea that the dipole bound state can provide an efficient doorway for attachment into the valence state.¹³ In the RET experiments reported previously for nitromethane^{10,11} and to be reported herein for nitroethane, the ion core stabilizes (i.e., removes rovibrational energy) the anion allowing it to become long lived or stable.

Herein, we present experimental and theoretical adiabatic electron affinities and vertical detachment energies, respectively, for the neutral and anionic forms of nitroethane and its clusters. We then use these energetic quantities to extract stepwise solvation energies for adjacent cluster sizes and as input into algorithms to determine the lifetime for the anions of nitroethane, nitrobenzene, and nitromethane. Comparisons of the autodetachment lifetimes are made between nitroethane, nitromethane, nitrobenzene, and deuterated nitrobenzene anions formed from thermal electron attachment. In addition, RET reactions with nitroethane are reported, which provides evidence for electron transfer into both dipole-bound and valence-bound anion states. The data demonstrate new features of the dipole-valence anion RET spectra which were also present in our previous study of nitromethane, but not commented upon, namely, a pronounced Rydberg angular momentum ℓ dependence on the distribution of n^* leading to anion formation.

II. METHODS

A. Photoelectron spectroscopy

Negative ion PES was used to measure the electron affinities and vertical detachment energies (VDEs) of $(\text{C}_2\text{H}_5\text{NO}_2)_n$, $n=1-5$ and their anions, respectively. Anion PES is conducted by crossing a mass-selected beam of negative ions with a fixed-frequency photon beam and energy-analyzing the resultant photodetached electrons. The photo-detachment process is governed by the relationship

$$h\nu = \text{EBE} + \text{EKE}, \quad (1)$$

where $h\nu$ is the photon energy, EBE is the electron binding energy, and EKE is the electron kinetic energy. Essentially, the photon energy is subdivided into the transition energy needed to take the anion to a particular vibronic state of its neutral counterpart, i.e., EBE, and the kinetic energy of the electron, i.e., EKE. Since photodetachment is an instantaneous process, the Franck–Condon overlap of the anion and neutral wavefunctions is reflected in the VDE. The VDE is the EBE of the maximum in the broadened photoelectron spectral profile, and as such, it is a well-defined quantity.

When there is good Franck–Condon overlap between the lowest vibrational level of the anion (v'') and the lowest vibrational level of its corresponding neutral (v'), the photoelectron spectrum also provides information about the adiabatic (thermodynamic) electron affinity of the neutral species. When the spectral profile is vibrationally resolved, an assignment of the spectrum can identify the $v''=0 \rightarrow v'=0$ transition. For this transition, its EBE value is equal to the adiabatic electron affinity (EA_a). When the profile is unresolved, however, the determination of EA_a is more approximate. If the anions were to be cold, i.e., if only $v''=0$ were occupied, then the low EBE threshold value of the spectrum would equal the EA_a value. However, since anions are often generated at significant temperatures, the first few vibrational levels of the anions may also be occupied, leading to some photoelectron intensity at EBE values less than that corresponding to the EA_a , i.e., due to hot bands.

The apparatus used in this work consists of a source for generating anions, a magnetic sector for mass analysis and mass selection, an argon ion laser operated intracavity as the photon source, and a hemispherical electron energy analyzer. The mass analyzer/selector has a mass resolution of ~ 500 , and the electron energy analyzer has a resolution of 28 meV. All photoelectron spectra reported here were recorded with 2.540 eV photons and calibrated against the photoelectron spectrum of O^- .¹⁴ The apparatus has been described previously.¹⁵

Nitroethane and its homogeneous cluster anions were generated in a supersonic expansion nozzle-ion source which was biased at -500 V. Nitroethane was placed inside the stagnation chamber of the source and was coexpanded with argon [35 psi (gauge)] through a 17 μm orifice into vacuum. Negative ions were formed by injecting electrons from a biased filament into the expanding jet, where a microplasma was formed with the help of an external magnetic field. Negative ions were then extracted into the beam line of the apparatus and subsequently mass selected so that the anions

of interest could be photodetached. Homogeneous molecular and cluster anions, $(\text{C}_2\text{H}_5\text{NO}_2)_n^-$, $n=1-8$, were observed, but only ions with $n=1-5$ were formed in sufficient abundance for the PES experiments.

B. Rydberg electron transfer

The experimental arrangement used to study RET to nitroethane is essentially identical to that employed previously.^{11,16} Briefly, light from a Nd:YAG (yttrium aluminum garnet) (Continuum Powerlite) laser pumped dye laser (Quanta Ray PDL-2) is directed antiparallel along an atomic beam of rubidium atoms. The dye laser is used to excite the rubidium atoms to n_s and n_d states using nonresonant two-photon absorption. The excited Rydberg atom beam is crossed with a pulsed nozzle jet (RM Jordan PSV model C-211) containing nitroethane and argon situated between the plates of a time-of-flight mass spectrometer (TOF-MS). The rubidium source was held at $\sim 170^\circ\text{C}$ and is housed in a separate chamber ~ 30 cm from the ion source region. The rubidium source, nozzle source, and TOF-MS flight tube regions are all separately pumped by three turbomolecular pumps. The negative ions formed during an interaction time of $\sim 2 \mu\text{s}$ are pulsed down the flight tube of a 1 m TOF-MS. The ions were detected with an electron multiplier employing three channel plates each having ~ 900 V applied across them and displayed on a LeCroy digital oscilloscope and averaged by a boxcar averager (Stanford Research Systems, model SR250). The data were recorded and treated by a data acquisition computer program written in LABVIEW. The nitroethane sample was purchased from Sigma-Aldrich Chemical and was used without purification.

C. *Ab initio* methods

As a complement to the experimental work, the electron binding properties of nitroethane, nitromethane, and the nitromethane dimer were also investigated computationally. Three sets of *ab initio* calculations were performed. First, the VDE and adiabatic electron affinity (EA_a) associated with the valence states of nitromethane and nitroethane were computed using second-order Moeller–Plesset perturbation theory (MP2) and coupled cluster theory with single and double substitutions (CCSD) as well as CCSD with a perturbation correction for triple substitutions [CCSD(T)]. Using these methods, the VDE and EA_a are computed as the difference of the total energies of neutral and anion. The basis sets used in these calculations were Dunning's augmented correlation-consistent double- ζ and triple- ζ sets (aug-cc-pVDZ and aug-cc-pVTZ),¹⁷ and the geometries and vibrational frequencies were computed with the MP2 method using the aug-cc-pVDZ basis. Second, the vertical electron affinity (VEA) values of nitromethane and nitroethane, that is the EBEs associated with the dipole-bound anion states, have been computed using the same Δ -methods as described above. Moreover these VEA values have been computed directly using the Koopmans's theorem (KT) approximation and the equation-of-motion CCSD (EOM-CCSD) methods. The electron density associated with the dipole-bound state is very diffuse, and to compute the VEA the aug-cc-pVDZ

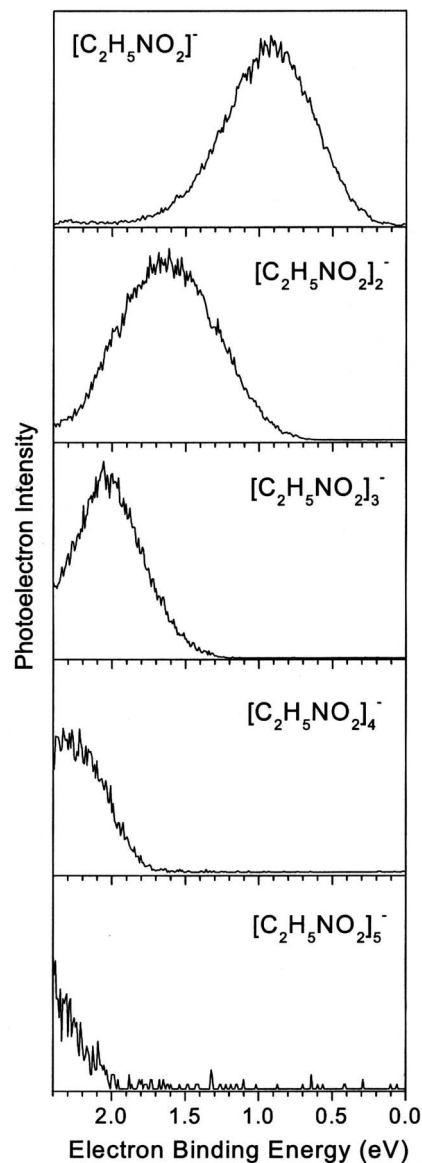


FIG. 1. PES of the nitroethane anion and its cluster anions.

set was augmented with a $5s5p5d$ basis set centered at the carbon atom attached to the nitro group. This basis set was created by adding first sp sets and then d sets to the aug-cc-pVDZ set (even-tempered exponents starting from the smallest respective exponents of the aug-cc-pVDZ set, scaling factor of 3.5), until the computed electron affinity was converged. Third, the VDE and EA_a values of the nitromethane dimer were studied. For these calculations, the geometries of monomers and dimers were optimized at the MP2 level using Pople's 6-31+G** basis set,¹⁸ and at the optimized geometries the energy was recomputed using the aug-cc-pVDZ set. Core electrons were not frozen in any of the calculations, and for all calculations the Mainz–Austin–Budapest version of the ACES II code¹⁹ was used.

III. EXPERIMENTAL RESULTS

The photoelectron spectra of the valence anion of nitroethane and its homogeneous cluster anions are shown in Fig. 1. The spectrum for the monomer anion exhibits a maxi-

TABLE I. Experimentally determined VDE and EA_a for anionic and neutral forms of nitroethane and its clusters, respectively.

Species	VDE (eV)	EA_a (eV)
$(C_2H_5NO_2)^-$	0.92 ± 0.1	0.3 ± 0.2
$(C_2H_5NO_2)_2^-$	1.63 ± 0.1	0.9 ± 0.2
$(C_2H_5NO_2)_3^-$	2.04 ± 0.1	1.5 ± 0.2
$(C_2H_5NO_2)_4^-$	2.3 ± 0.1	1.9 ± 0.2
$(C_2H_5NO_2)_5^-$...	2.1 ± 0.4

mum at 0.92 eV and a threshold at ~ 0.2 eV. Thus, the VDE value of the nitroethane anion is 0.92 eV. While there is the suggestion of weak vibrational structure in the spectrum, an expanded view of the threshold region fails to reveal a clear peak for assignment to a $0 \leftarrow 0$ transition. Based on the location of its threshold and patterns typical of anion photoelectron spectral profiles, we assign its adiabatic electron affinity (EA_a) value as lying in the vicinity of 0.2–0.4 or 0.3 ± 0.2 eV. The spectra for the nitroethane cluster anions similarly exhibit little discernible vibrational structure and thus the same assignment procedure applies to the electron affinities of these clusters. The nitroethane cluster anions form stable singly charged anions with increasing EBEs (electron affinities of their neutral counterparts) with increasing numbers of molecules per cluster. The adiabatic electron affinities (EA_a) and VDE derived from these spectra are

summarized in Table I. Generally, the extracted VDE values are more reliable than the extracted EA_a values.

Figure 2(a) shows the RET ion signal for the nitroethane negative ion as a function of the effective principle quantum number for both the n_s and n_d series. Unlike other RET spectra reported previously (see, e.g., Ref. 16), this plot demonstrates that the n_s and n_d profiles are distinctly different, with the s states peaking at a lower n^* .^{11,16} A similar dependence was evident in the previous study¹¹ of nitromethane as well as in a follow-up report²⁰ but was not commented upon. The Rydberg charge exchange spectrum for nitroethane also extends over a much wider range of n^* than other RET dipole anion spectra. The RET spectra extends to very high n^* as would be expected for attachment into the valence anion state; however, the peak at low n^* is also very much broader than previously observed for pure dipole anion formation (i.e., for cases in which there is no lower lying valence anion state). The dynamic coupling of the dipole and valence anion is clearly affecting the observed n dependence of the RET. In the absence of the lower-lying valence state, anions formed in higher rotational states, which were present in the initially formed dipole bound anions, will autodetach before they can be detected. However, rapid dipole-valence anion coupling could act to stabilize the system through intermolecular charge transfer. The dipole-bound electron affinities (EA_a) for a large number of polar molecules has been estimated

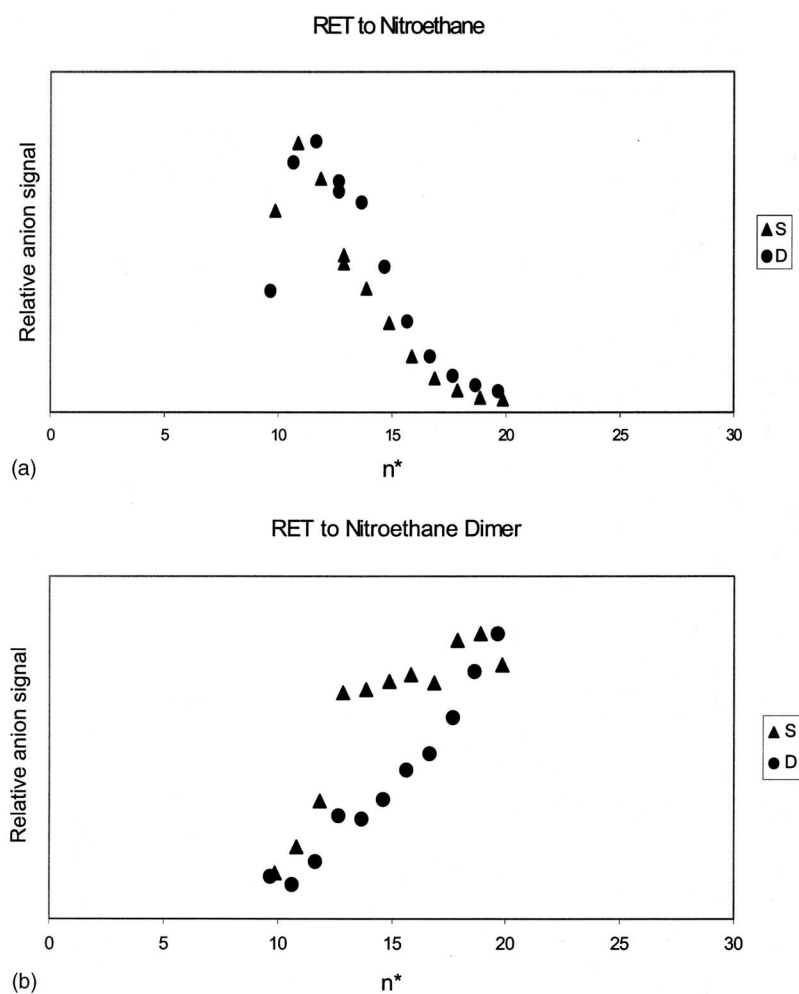


FIG. 2. RET spectra for nozzle-jet expanded nitroethane (a) and its dimer (b) showing ion signals for both n_s and n_d charge transfer.

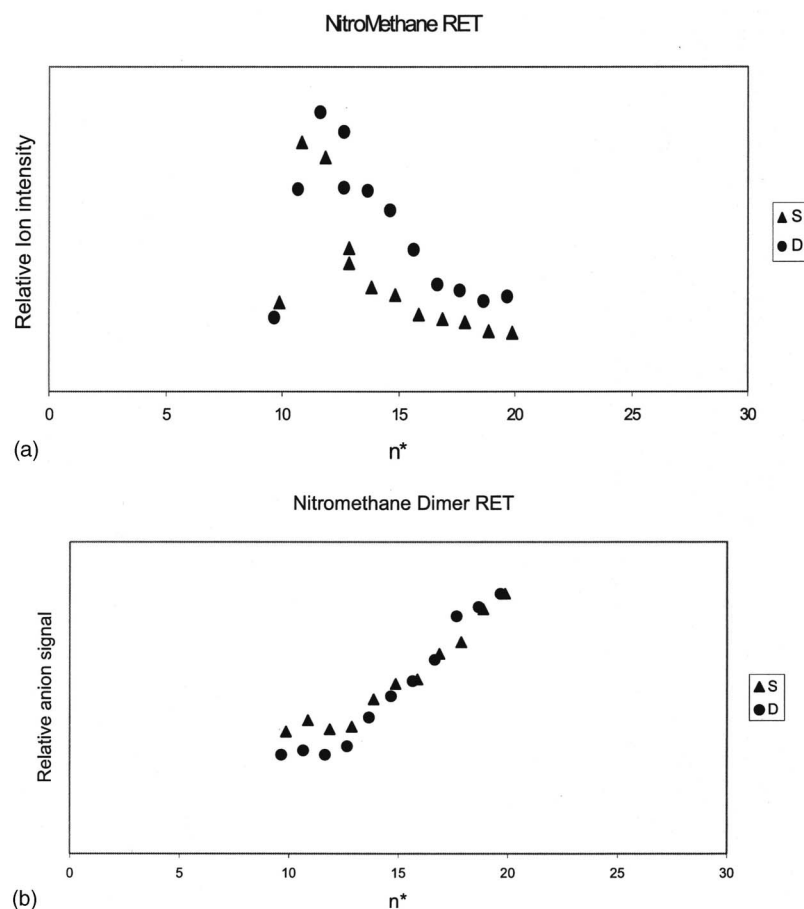


FIG. 3. RET spectra for nozzle-jet expanded nitromethane (a) and its dimer (b) showing ion signals for both n_s and n_d charge transfer.

using the empirical expression derived from the curve crossing model of Desfrancois,²¹ $EA_a = 23/(n_{\max}^{*2.8})$, where n_{\max}^* represents the effective quantum number corresponding to the maximum in the RET spectra.²¹ Using this simple model, and making the assumption that the valence state does not perturb this analysis, we obtain EA_a values of 28.47 and 25.28 meV, for the n_s and n_d profiles, respectively. Similar values were found from the n_s and n_d profiles for RET of nitromethane. These values are somewhat higher than those from previously reported studies^{11,20} due to their inclusion of the n_f series which gives a higher n_{\max}^* than the s or d states and thus a lower electron affinity. However, the broad n^* observed and the marked ℓ dependence places this analysis into uncertainty.

RET spectra were also recorded for the nitroethane dimer and is shown in Fig. 2(b). One notes a steady increase of dimer ion RET signal as the principal quantum number increases. This is indicative of low-energy electron attachment into a valence bound anion via capture into a nuclear excited Feshbach resonance. In this case, the increased density of vibrational states along with the larger electron affinity may allow for a long-lived negative ion state, which does not require vibrational relaxation via interactions with the Rydberg ion core as in the case of the monomer.

For comparison, we have briefly re-examined RET for the nitromethane monomer and nitromethane dimer and the results are shown in Fig. 3. There is a clear dependence of the RET cross section on the angular momentum state of the Rydberg electron, with the peak occurring at larger n^* for the

n_d Rydberg series. The dimer cross section shows a steady rise with increasing n^* , however, there is a hint of a peak in the region of n^* where the RET for the monomer peaks ($n^* \sim 12$). If real, it could be considered to be the result of a short range interaction of the Rydberg excited atom with the local dipole field of one of the nitromethane molecules making up the dimer. The RET spectra for nitroethane and nitromethane and their dimers are similar.

IV. AB INITIO RESULTS

In this section, electron attachment to nitromethane, nitroethane, and nitromethane clusters is studied theoretically. Both nitromethane and nitroethane can attach an electron in two fundamentally different states. First, both molecules have substantial dipole-moments, and can attach an electron into a diffuse dipole-bound state. Second, both molecules can bind an electron into a far more compact valence state mainly associated with attachment to the nitro group. At the geometry of the neutral molecules, only the dipole-bound states are stable, whereas the valence states correspond to metastable resonance states. However, the valence state is strongly stabilized when the planar nitro group of the neutrals is pyramidalized, and at the geometry of the valence anion the VDE associated with the valence state is substantial.

Computational results for the VEA associated with the dipole-bound states, and for the VDE and the EA_a associated with the valence states of nitromethane and nitroethane are

TABLE II. Computed VEA and dipole moments of nitromethane and nitroethane. The aug-cc-pVDZ set augmented with a diffuse $5s5p5d$ set centered at the carbon atom attached to the nitro group has been used. The computed VEA values do not include zero point energies.

	Nitromethane	Nitroethane
	Vertical electron affinity (meV)	
KT	6.3	4.7
SCF	6.7	5.0
MP2	5.4	4.5
CCSD	10.1	9.5
CCSD(T)	8.4	7.9
EOM-CCSD	15.3	13.8
	Dipole moment (D)	
Experimental ^a	3.49	3.23
MP2	3.46	3.64

^aFrom reference 24.

collected in Tables II and III. Before discussing the results in detail, let us point out the striking similarity of the electron attachment properties of nitromethane and nitroethane. At all levels of theory, the two molecules are predicted to possess virtually identical VEAs, VDEs, and EA_a s. That is, we can conclude that the electron attachment properties of the two molecules are dominated by the nitro group, while the effect of the organic side chain is minor.

The VEA of the two molecules is the EBE associated with the dipole-bound state, and it is essentially determined by the dipole moment of the neutral framework. Both molecules have dipole moments of about 3.5 D (Table II). The experimental and calculated values for the dipole moments agree very nicely for nitromethane, while for nitroethane the agreement is somewhat less satisfactory. In particular, the experimental trend is that nitroethane has a somewhat smaller dipole moment than nitromethane, whereas the computed trend predicts the opposite. Be this as it may, the difference of the two dipole moments is small, and the computations predict that both molecules possess a dipole-bound state with a binding energy of roughly 8 meV at the CCSD(T) level (Table II), which is presumably our best result. As expected for a dipole-bound state, including high-order electron correlation beyond MP2 is vital for describing the distribution of the loosely bound excess electron.²⁵ Comparing the two molecules, the VDE of nitromethane is predicted to be slightly larger than that of nitroethane (by about

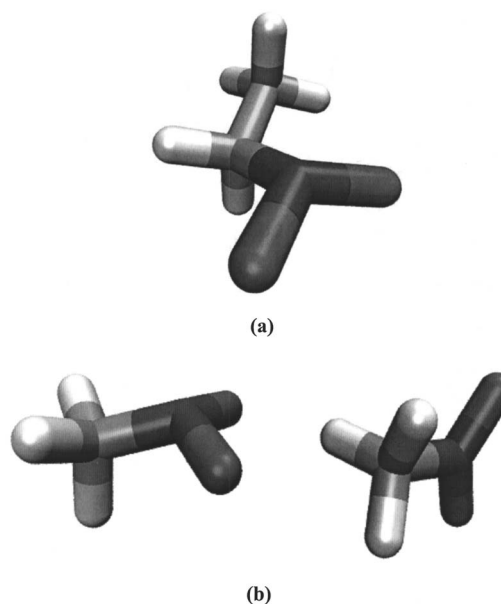


FIG. 4. (a) Geometrical structure of the nitroethane valence anion. The C_1 symmetrical conformer optimized using the MP2 method and aug-cc-pVDZ basis is shown. Carbon atoms are turquoise, Nitrogen atoms are blue, Oxygen atoms are red, and Hydrogen atoms are white. (b) Geometrical structure of the nitromethane dimer anion. The dimer forms only a type-I anion, that is, the electron is attached to one monomer unit (here the left-hand side monomer) and the second monomer solvates the monomer anion. The atoms are colored as in (a).

1 meV), despite the opposite trend in the computed dipole moments. This trend of the binding energies can be interpreted in terms of an excluded volume effect. Loosely speaking, the excess electron preferably occupies the space close to the positive end of the molecular dipole, however, for nitroethane, this space is partly blocked by the additional methyl group resulting in a slightly smaller VEA.

In the valence state of both anions, the nitro group has a trigonal-pyramidal geometry. The nitromethane anion has a staggered geometry with C_s symmetry, and the nitromethane anion has two staggered conformers with C_s and C_1 symmetry, respectively, where the C_1 symmetrical conformer [Fig. 4(a)] is slightly lower in energy ($\Delta E < 20$ meV at the MP2 level). The computed values in Table III all refer to the more stable C_1 conformer shown in Fig. 4(a). Regarding the VDE and EA_a values listed in Table III, three comments are in order. First, high-order electron-correlation effects are

TABLE III. Computed vertical detachment energies and adiabatic electron affinities of the nitromethane and nitroethane molecules. Negative EA_a values imply that the anion is less stable than the neutral. Vibrational zero-point corrections are not included.

	VDE (eV)			Adiabatic electron affinity (eV)		
	$\text{CH}_3\text{-NO}_2^a$	$\text{CH}_3\text{-NO}_2^b$	$\text{C}_2\text{H}_5\text{-NO}_2^a$	$\text{CH}_3\text{-NO}_2^a$	$\text{CH}_3\text{-NO}_2^b$	$\text{C}_2\text{H}_5\text{-NO}_2^a$
SCF	1.50	1.49	1.47	-0.03	-0.08	-0.05
B3LYP	1.18	...	1.14	0.41	...	0.40
MP2	0.55	0.68	0.56	-0.26	-0.24	-0.25
CCSD	1.10	1.24	1.12	0.13	0.13	0.14
CCSD(T)	0.86	0.99	0.88	0.04	0.05	0.05

^aaug-cc-pVDZ basis set.

^baug-cc-pVTZ basis set.

again crucial as the Δ SCF and Δ MP2 results noticeably deviate from the Δ CCSD(T) values, and the same is true for B3LYP calculations. Second, more flexible basis sets recover more electron correlation, and therefore the computed VDE tends to increase somewhat when more flexible basis sets are employed. Interestingly, for the EA_a this basis set effect is tiny. Third, the results for nitromethane and nitroethane are virtually identical. Thus, based on the CCSD(T) result obtained with the aug-cc-pVTZ basis set, we predict for both molecules a VDE of about 1.0 eV, and for the EA_a a small positive value of about 50 meV. Taking vibrational zero-point effects computed within the harmonic approximation at the MP2 level into account, the EA_a is increased by about 70 meV for nitromethane and by about 80 meV for nitroethane. Thus, we predict an EA_a value between 0.1 and 0.2 eV for both molecules.

In order to make the terms “diffuse dipole-bound state” and “compact valence state” more transparent, the orbitals associated with the excess electron in the dipole-bound and valence states are compared in Figs. 5(a) and 5(b). Of course, the very notion of an orbital for the excess electron exists only at the one-electron level, but it is nevertheless instructive to consider. For the dipole-bound state, electron correlation effects have a dramatic influence on the distribution on the excess electron, and thus the natural orbital of the EOM-CCSD density associated with the excess electron (occupation number close to 1) is depicted [Fig. 5(a)]. In contrast, for the valence anion the singly occupied Hartree–Fock orbital is expected to give an acceptable description of the density, and it is shown in Fig. 5(b). As can be seen in the figures, for the valence anion the isosurface enclosing 90% of the electron density has the same spatial extent as the molecule itself, and integrating the density is enclosed in the volume defined by the van der Waals radii of the atoms yields 95%. Thus, in the valence state, the excess electron is localized on the molecular framework similar to usual valence electrons. In contrast, the 90% contour of the dipole-bound electron dwarfs the molecule, and less than 0.5% of the density is enclosed in the van der Waals volume of the atoms. Thus, the dipole-bound state has essentially Rydberg-like character with almost negligible amounts of density close to the molecular framework.

Finally, we consider dimer anions. Since nitromethane and nitroethane have practically identical electron attachment properties, for computational practicability, we investigated the nitromethane dimer anions. For other dimer anions including $(CO_2)_2^-$, $(COS)_2^-$, $(CS_2)^-$, and $(H_3CCN)_2^-$, it is well established that valence anions exist in two forms. Type-I anions that consist of a monomer anion solvated by a neutral monomer, and type-II anions that consist of dimer anions, that is, there is a chemical bond between the monomer units and the dimer anion is a new chemical species.^{26–28} We searched for both types of anion for nitromethane, but could only find a type-I structure that is shown in Fig. 4(b). Using geometries optimized at the MP2/6-31+G** level, and energies evaluated at the MP2/aug-cc-pVDZ level, the dissociation energy of the dimer anion is predicted to be 0.87 eV. At the same level, the increase in VDE in going from the monomer to the dimer anion is predicted to be 0.76 eV.

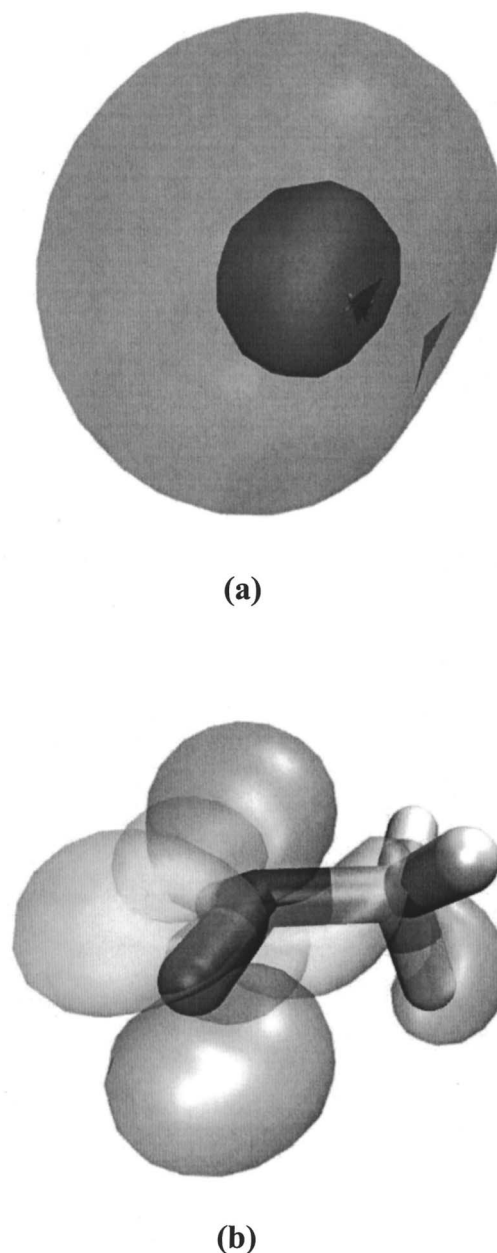


FIG. 5. (a) Distribution of the excess electron in the dipole-bound state of the nitromethane anion. Two isosurface of the EOM-CCSD natural orbital describing the excess electron are shown. The outer isocontour encloses 90%, the inner iso-surface encloses 50% of the electron density. Both isosurface dwarf the molecular framework, the atoms are colored as in Fig. 4(a). (b) Distribution of the excess electron in the valence state of the nitromethane anion. The isosurface of the singly occupied Hartree-Fock orbital enclosing 90% of the electron density is shown, and the atoms are colored as in Fig. 4(a).

Thus, from the best VDE, we have for the monomer and the computed VDE change between monomer and dimer, we can predict a VDE of about 1.8 eV for the nitromethane dimer anion. For the nitroethane dimer, the stabilization provided by the solvating monomer may be somewhat different, but should have the same order of magnitude.

V. DISCUSSION AND CONCLUSIONS

Electron attachment properties of the nitroethane molecule and nitroethane clusters have been investigated using

PES, RET, and *ab initio* computations. RET addresses the VEA associated with the dipole bound state of the molecules. Both the experimental and theoretical results show that nitroethane behaves similarly to nitromethane. In both cases, RET is most efficient in the same n^* region between $n^* = 10$ and $n^* = 15$, with RET from *s* states peaking at $n^* = 11$ and RET from *d* states peaking at $n^* = 12$. The same similarity between the two molecules is found in high level *ab initio* calculations that predict VEAs of about 8 meV for both molecules. However, the *ab initio* results are at odds with the VEA derived from the RET spectra using a one-dimensional curve crossing model.

PES yields the VDE and an estimate for the EA_a associated with the valence state of the nitroethane anion. The computed VDE value of 0.88 eV (at the highest level of theory employed) is in good agreement with the peak maximum (and thus the VDE) of 0.92 ± 0.1 eV in the photoelectron spectrum of nitroethane. For the VDE of the nitroethane dimer anion, theory predicts 1.8 eV, whereas experiment finds 1.6 eV. The computed values of VDE for nitromethane also agree well with the experimental VDE values reported in Ref. 11. While there is more uncertainty in our experimental EA_a value of 0.3 ± 0.2 eV for nitroethane, it too is in satisfactory agreement with our calculations which suggest an EA_a value between 0.1 and 0.2 eV.

Apart from the electron attachment properties of the nitroethane monomer, the experimental results provide information on the microsolvation in nitroethane clusters. Both the PES experiments and the *ab initio* calculations suggest that the observed cluster anions are so-called type-I clusters, that is, the excess electron is attached to a single monomer unit and the other nitroethane molecules solvate this anion. The shifts between the photoelectron spectra of adjacent size, nitroethane cluster anions can then be used to extract stepwise (sequential) nitroethane anion-molecule interaction energies.

In general, energetic relationships between solvated cluster anions, $X^-(Y)_n$, and their corresponding neutrals, $X(Y)_n$, allows one to relate electron affinities, ion-neutral dissociation energies, and neutral-neutral dissociation energies via the identities:

$$EA[X(Y)_n] = EA[X] + \sum_{m=0}^{n-1} D[X^-(Y)_m \cdots Y] - \sum_{m=0}^{n-1} D_{WB}[X(Y)_m \cdots Y]. \quad (2)$$

and

$$EA[X(Y)_n] = EA[X(Y)_{n-1}] + D[X^-(Y)_{n-1} \cdots Y] - D_{WB}[X(Y)_{n-1} \cdots Y], \quad (3)$$

where $EA[X(Y)_n]$ is the adiabatic electron affinity of $X(Y)_n$, $D[X^-(Y)_{n-1} \cdots Y]$ is the ion-neutral dissociation energy for the loss of a single solvent molecule, Y , from the cluster anion, $X^-(Y)_n$, and $D_{WB}[X(Y)_{n-1} \cdots Y]$ is the analogous neutral cluster, weak bond, dissociation energy for the loss of a single solvent molecule, Y , from the neutral cluster, $X(Y)_n$. It is evident from Eq. (2) that electron affinities should increase

TABLE IV. Stepwise solvation energies and ion-solvent interaction energies for nitroethane and nitromethane. Neutral dissociation energies were taken to be zero. All values are in eV.

Nitroethane	EA	SE _{step} (this work)	$-\Delta H_{n-1,n}^o$ (Wincel)
$(C_2H_5NO_2)^-$	0.3
$(C_2H_5NO_2)_2^-$	0.9	0.6	...
$(C_2H_5NO_2)_3^-$	1.5	0.6	0.63 ^b
$(C_2H_5NO_2)_4^-$	1.9	0.4	0.59 ^b
$(C_2H_5NO_2)_5^-$	2.1	0.2	0.52 ^b
Nitromethane			
$(CH_3NO_2)^-$	0.26 ^a
$(CH_3NO_2)_2^-$	0.92 ^a	0.66 ^a	0.66 ^c
$(CH_3NO_2)_3^-$	1.50 ^a	0.58 ^a	0.56 ^c
$(CH_3NO_2)_4^-$	0.45 ^c
$(CH_3NO_2)_5^-$	0.37 ^c

^aReference 11.

^bReference 22.

^cReference 23.

with cluster size as additional solvent molecules stabilize the excess charge on the anion. The stepwise (sequential) solvation (stabilization) energy, SE_{step} , for $X^-(Y)_{n-1}$ gaining another Y solvent molecule is $-D[X^-(Y)_{n-1} \cdots Y]$. Such incremental solvation stabilization energies typically diminish as the number of solvent molecules increases.

In the case of nitroethane cluster anions, the photoelectron spectral profile of the molecular anion, $C_2H_5NO_2^-$ is largely maintained throughout the subsequent cluster series, $(C_2H_5NO_2)_n^-$, suggesting that the excess charge is more or less localized on a single nitroethane molecular unit and implying that $(C_2H_5NO_2)_n^-$ can be written as $(C_2H_5NO_2)^-(C_2H_5NO_2)_{n-1}$, where $C_2H_5NO_2^-$ assumes the role of X^- and $C_2H_5NO_2$ takes on the role of Y in the equations above. In this context, $X(Y)_n$ becomes nitroethane cluster size, $n+1$, and $X(Y)_{n-1}$ becomes nitroethane cluster size n .

Thus, through Eq. (3), one sees that the difference in electron affinities between adjacent size nitroethane clusters (essentially the spectral shift between them) is equal to $D[X^-(Y)_{n-1} \cdots Y] - D_{WB}[X(Y)_{n-1} \cdots Y]$, or if the symbol, NE is used to represent nitroethane, this difference can be written as $D[NE^-(NE)_{n-1} \cdots NE] - D_{WB}[NE(NE)_{n-1} \cdots NE]$. The neutral-neutral interaction energy, $D_{WB}[X(Y)_{n-1} \cdots Y]$, is usually significantly smaller than the ion-neutral interaction energy, $D[X^-(Y)_{n-1} \cdots Y]$. In fact, since nitroethane is a high vapor pressure liquid at room temperature, its neutral-neutral interaction strength is likely to be particularly weak and was taken to be zero. Thus, the difference in electron affinities between adjacent size nitroethane clusters is a good approximation to $D[NE^-(NE)_{n-1} \cdots NE]$, i.e., to $-SE_{step}$.

Table IV displays the stepwise stabilization energies, SE_{step} , for nitroethane clusters measured in this work along with those reported by Wincel²² who utilized high pressure mass spectrometry and van't Hoff plots to determine enthalpy changes, $-\Delta H_{n-1,n}^o$, for stepwise solvation processes of the type, $X^-(Y)_{n-1} + Y \rightarrow X^-(Y)_n$. Along with results for nitroethane, Wincel²³ also reported values for nitromethane

which are also included in Table IV along with those reported in our earlier study.¹¹ For both nitroethane and nitromethane, the stepwise solvation energies determined by the two studies are in reasonable agreement for the two smallest, $n-1 \rightarrow n$ comparisons that were available. Our calculation's prediction of ~ 0.8 eV for the dissociation energy of the nitroethane dimer anion is in reasonable accord with our experimentally derived SE_{step} value of 0.6 eV. The size of the combined error bars made impractical the extraction of neutral-neutral interaction energies based on a comparison of two studies.

Finally, we examine the question of the lifetime of negative ions formed by unimolecular electron attachment for relatively small molecules (e.g., nitromethane and nitroethane) and estimate lifetimes in the range of 10^{-6} – 10^{-9} s. The nitroethane and nitromethane negative ions studied using PES were produced by slow electron attachment into a short-lived $C_2H_2NO_2^{*-}$ nuclear excited Feshbach resonance. Collisions with other molecules remove sufficient internal energy (vibrational quanta) leading to stable negative ions. Subsequent collisions relax the anions to roughly ~ 300 K internal rovibrational energy. A comparison of the lifetimes of these three nitrocompounds provides interesting insight into negative ion lifetimes and their importance in mass spectrometry.

In order to estimate the lifetimes of nitroethane, nitromethane, nitrobenzene and d-nitrobenzene negative ions formed by slow electron attachment, we utilized the quasi-equilibrium theory (QET) arguments introduced by Compton *et al.*⁸ and Klots²⁹ in which detailed balancing is used to relate the electron attachment rate and autodetachment rate. In its simplest embodiment the autodetachment lifetime τ for attachment of electrons with velocity v for an attachment cross section $\sigma(v)$ is given by

$$\tau = [\rho(E^*)^- / \rho_{\text{em}}][1/v\sigma(v)], \quad (4)$$

where $\rho(E^*)^- / \rho_{\text{em}}$ is the ratio of densities of states of the negative ion having a total energy E^* to that of the density of states for the initial electron-molecule system. E^* is the excess vibrational energy of the negative ion (electron affinity plus incident electron energy plus any initial vibrational energy in the neutral before attachment). Effects of rotational motion are not addressed in this treatment and all vibrations are considered to be effective (equipartition of energy). The density of states for the negative ion, $\rho(E^*)^-$, is calculated by a modified version of the Marcus-Rice QET expression proposed by Whitten and Rabinovitch.³⁰

Calculation of the autodetachment lifetime for a vibrationally excited negative ion requires knowledge of the vibrational frequencies of the neutral and anion, attachment cross section and adiabatic electron affinity. Frequencies of neutral and negative ions for nitroethane, nitromethane, nitrobenzene and d-nitrobenzene were calculated using Density Functional Theory and aug-cc-pVDZ basis set using the GAUSSIAN-G03 package.³¹ Experimental values of electron affinities are used in the calculations. The calculated lifetime is quite sensitive to the adiabatic electron affinity, therefore in case of nitroethane we have attempted to calculate the lifetime for three different electron affinities (calculated and ex-

TABLE V. Lifetime calculations using experimental and computed electron affinities, electron attachment rates, and calculated vibrational frequencies for the nitro-containing molecular negative ions formed by thermal electron attachment. Due to uncertainty of nitroethane adiabatic electron affinity, lifetime has been calculated for three different adiabatic electron affinities. (N is the number of vibrational degrees of freedom).

Molecule	N	Electron affinity (eV)	Lifetime(s)
			B3LYP/aug-cc-pVDZ
Nitrobenzene	36	1 ^a	1.24×10^{-2}
Deuterated Nitrobenzene	36	0.99 ^b	2.13×10^{-2}
Nitroethane	24	0.4 ^c	9.39×10^{-8}
		0.2 ^c	3.05×10^{-9}
		0.14 ^c	8.79×10^{-10}
Nitromethane	15	0.26 ^d	1.32×10^{-9}

^aReference 10.

^bWe assume the experimental electron affinity of deuterated nitrobenzene to be the same as nitrobenzene with a zero point energy correction.

^cThis work.

^dReference 11.

perimental values) as shown in Table V. Absolute cross sections for associative electron attachment are available for nitrobenzene.⁸ However, there are no values of cross sections for nitroethane and nitromethane, thus we use the nitrobenzene cross section for all of our calculations. In this context, Lunt *et al.*⁶ suggest that the total cross sections for all of these molecules are approximately the same providing some support for the assumed cross sections.

Table V shows the lifetimes predicted for the negative ions based upon the simple QET [Eq. (4)]. One notes very long lifetimes for nitrobenzene due to the larger electron affinity and greater number of degrees of freedom. The calculated lifetime exceeds the experimental value. This appears to be the situation for many long-lived negative ions previously reported (see Refs. 32 and 33). However, there are many other molecules for which QET and experiment are in agreement. Lifetimes of negative ions have been addressed in a recent study by Cannon *et al.*³² and in a review by Mirsaleh-Kohan *et al.*³³ As found for the case of nitrobenzene and other anions, the measured lifetimes can be somewhat shorter than that calculated from QET. However, it is interesting to note that the QET theory does qualitatively agree with the isotope effect previously reported on the autodetachment lifetime⁹ for nitrobenzene and deuterated nitrobenzene. The important subject of negative ion lifetimes is in need of considerably more experimental and theoretical attention. It is quite possible that QET does not apply in all cases and some vibrations are "silent" in electron attachment.

The lifetimes predicted for nitroethane and nitromethane are much too short lived to be seen in a mass spectrometer due solely to unimolecular electron attachment which is in accord with experimental observations. The ions studied in the photodetachment experiments reported herein are a result of collisional stabilization (vibrational cooling) of these short lived anions. The small electron affinity found for nitroethane presents an interesting problem in the description of the autodetachment lifetime assuming QET. The electron affinity is smaller than some of the vibrational frequencies predicted for the nitroethane anion and these frequencies would

not be available to accommodate the excess energy. Thus the autodetachment lifetimes presented in Table V may be too large as a result of the small adiabatic electron affinity predicted for nitroethane. Specifically, we note that some of the vibrational energies for this anion may be smaller than the electron affinity reported or calculated for nitroethane. For example, if the lower limit value of 0.14 eV (also the calculated value) is adapted for the electron affinity for nitroethane, then 13 of the vibrational energies are *greater than* the electron affinity. In this case these frequencies should not be counted in the density of states since they cannot be excited under electron attachment. In this case the lifetime will be decreased considerably below that expected from QET in which all of the degrees of freedom are assumed to be effective.

ACKNOWLEDGMENTS

This material is based upon work supported by the National Science Foundation under Grant Nos. CHE-0517337 (K.H.B.) and CHE-0352398 (R.N.C.).

- ¹A. Pelc, W. Sailer, S. Matejcek, P. Scheier, and T. D. Märk, *J. Chem. Phys.* **119**, 7887 (2003).
- ²S. Tsuda, A. Yokohata, and M. Kaway, *Bull. Chem. Soc. Jpn.* **42**, 607 (1969).
- ³K. Jäger and A. Henglein, *Z. Naturforsch. A* **22A**, 700 (1967).
- ⁴J. Pacansky, N. S. Dalal, and P. S. Bagus, *Chem. Phys.* **32**, 183 (1978).
- ⁵K. A. Peterson and M. Gutowski, *J. Chem. Phys.* **116**, 3297 (2002).
- ⁶S. L. Lunt, D. Field, J.-P. Ziesel, N. C. Jones, and R. J. Gulley, *Int. J. Mass. Spectrom.* **205**, 197 (2001).
- ⁷J. A. Stockdale, F. J. Davis, R. N. Compton, and C. E. Klots, *J. Chem. Phys.* **60**, 4279 (1974).
- ⁸R. N. Compton, L. G. Christophorou, G. S. Hurst, and P. W. Reinhardt, *J. Chem. Phys.* **45**, 4634 (1966).
- ⁹W. T. Naff, R. N. Compton, and C. D. Cooper, *J. Chem. Phys.* **54**, 212 (1971).
- ¹⁰C. Desfrancois, V. Periquet, S. A. Lypustina, T. P. Lippa, D. W. Robinson, K. H. Bowen, H. Nonaka, and R. N. Compton, *J. Chem. Phys.* **111**, 4567 (1999).
- ¹¹R. N. Compton, H. S. Carman, C. Desfrancois, H. Abdoul-Carime, J. P. Schermann, J. H. Hendricks, S. A. Lypustina, and K. H. Bowen, *J. Chem. Phys.* **105**, 3472 (1996).
- ¹²C. Desfrancois, H. Abdoul-Carime, and J. P. Schermann, *Int. J. Mod. Phys. B* **10**, 1339 (1996); R. N. Compton and N. I. Hammer, in *Advances in Gas Phase Ion Chemistry*, edited by N. Adams and L. Babcock (Elsevier, New York, 2001), Vol. 4, pp. 257–259.
- ¹³T. Summerfeld, *Phys. Chem. Chem. Phys.* **4**, 2511 (2002).
- ¹⁴D. M. Neumark, K. R. Lykke, T. Andersen, and W. C. Lineberger, *Phys. Rev. A* **32**, 1890 (1985).
- ¹⁵J. V. J. V. Coe, J. T. Snodgrass, C. B. Freidhoff, K. M. McHugh, and K. H. Bowen, *J. Chem. Phys.* **84**, 618 (1986).
- ¹⁶N. I. Hammer, K. Diri, K. D. Jordan, C. Desfrancois, and R. N. Compton, *J. Chem. Phys.* **119**, 3650 (2003).
- ¹⁷T. H. Dunning, Jr., *J. Chem. Phys.* **90**, 1007 (1989).
- ¹⁸W. J. Hehre, R. Ditchfield, and J. A. Pople, *J. Chem. Phys.* **56**, 2257 (1972).
- ¹⁹J. F. Stanton, J. Gauss, J. D. Watts, P. G. Szalay, R. J. Bartlett, with contributions from A. A. Auer, D. B. Bernholdt, O. Christiansen, M. E. Harding, M. Heckert, O. Heun, C. Huber, D. Jonsson, J. Jusélius, W. J. Lauderdale, T. Metzroth, C. Michauk, D. P. O'Neill, D. R. Price, K. Ruud, F. Schiffmann, M. E. Varner, J. Vázquez, MAB-Aces II and the integral packages, J. Almlöf and P. R. Taylor, MOLECULE., P. R. Taylor, PROPS, and T. Helgaker, H. J. Aa. Jensen, P. Jørgensen, and J. Olsen, ABACUS. For the current version, see <http://www.aces2.de>.
- ²⁰R. N. Compton and N. I. Hammer, in *Advances in Gas-Phase Ion Chemistry*, edited by N. Adams and L. Babcock (Elsevier, New York, 2001), Vol. 4, pp. 257–291.
- ²¹C. Desfrancois, *Phys. Rev. A* **51**, 3667 (1995).
- ²²H. Wincel, *Int. J. Mass. Spectrom.* **232**, 185 (2004).
- ²³H. Wincel, *Int. J. Mass. Spectrom.* **226**, 341 (2003).
- ²⁴*CRC Handbook of Chemistry and Physics*, 79th ed. (CRC, Boca Raton, 1999).
- ²⁵M. Gutowski, P. Skurski, A. I. Boldyrev, J. Simons, and K. D. Jordan, *Phys. Rev. A* **54**, 1906 (1996).
- ²⁶S. H. Fleischman and K. D. Jordan, *J. Phys. Chem.* **91**, 1300 (1987).
- ²⁷A. Sanov, S. Nandi, K. D. Jordan, and W. C. Lineberger, *J. Chem. Phys.* **109**, 1264 (1998).
- ²⁸S. Barsotti, T. Sommerfeld, M.-W. Ruf, and H. Hotop, *Int. J. Mass. Spectrom.* **233**, 181 (2004).
- ²⁹C. E. Klots, *J. Chem. Phys.* **46**, 1197 (1967).
- ³⁰G. Z. Whitten and B. S. Rabinovitch, *J. Chem. Phys.* **38**, 2466 (1963).
- ³¹M. J. Frisch, G. W. Trucks, H. B. Schlegel, *et al.*, Gaussian 03, Revision C.02, Gaussian, Inc., Wallingford, CT, 2004.
- ³²M. Cannon, Y. Liu, L. Suess, F. B. Dunning, J. Steill, and R. N. Compton, *J. Chem. Phys.* **127**, 064314 (2007).
- ³³N. Mirsaleh-Kohan, W. D. Robertson, and R. N. Compton, *Mass Spectrom. Rev.* **27**, 237 (2008).